Surface Wave Modes of Printed Circuits on Ferrite Substrates

Hung-Yu Yang, *Member, IEEE,* Jesse A. Castaneda, *Member, IEEE,* and Nicolaos G. Alexopoulos, *Fellow, IEEE*

***Abstract*—Surface waves due to a current source on a grounded ferrite slab are investigated. Electromagnetic fields of the structure are in terms of a continuous plane wave spectrum. The spectrum of each field component is obtained numerically through the exponential-matrix method. The surface waves of the structure are extracted from the continuous spectrum by using the residue theorem and the method of steepest descent. Two types of surface waves are found and their properties are described. The surface wave modes found include dynamic surface wave modes which are closely related to the surface waves of a grounded dielectric slab, and magneto-static surface wave modes which are related to the solution of Laplace's equation for the magnetic potential.**

I. Introduction

GYROTROPIC materials (ferrites) exhibit magnetic anisotropy with the application of external dc magnetic fields. The permeability of the material is described in a tensor form, where its elements are determined by frequency of operation, ferrite saturation magnetization, and applied dc magnetic field [1], [2].

For an open geometry, circuit discontinuities introduce surface waves which contribute to the loss mechanism of the circuits. From an antenna point of view, electromagnetic fields due to a current source on a ferrite substrate are in the form of a continuous phase wave spectrum. The waves propagating laterally, which are often called surface waves, are essential to the characteristics of the printed circuit antenna [3].

Surface waves due to an infinite line source on an ferrite slab have been studied by a number of investigators [4]–[10]. The problem which they had studied is for fields with no variation in one of the planar directions. The surface waves are either TE or TM modes and are plane waves with an equi-phase plane perpendicular to the ground plane. The characteristic equations for both TE and TM modes are simple transcedental functions. Also, the propagation constant of the TM modes is the same as the TM modes of a dielectric substrate with the same ϵ_r. It had been found that there exist two types of surface wave modes. One is the magneto-static wave mode and the other is the dynamic surface wave mode which is related to the surface wave modes of a dielectric slab. The magneto-static waves have been found to exist only in a certain frequency range and only when the bias magnetic field is in the planar direction and perpendicular to the direction of wave propagation. The properties of magnetostatic surface waves due to a point source are discussed in [11], where magnetostatic equations instead of Maxwell's equations are solved. The analysis described in [11] is a simplified approach and can not account the dynamic surface wave modes. In this work, we study the surface waves due to an arbitrarily oriented current source on a ferrite substrate with bias magnetic field. The bias field can be in any direction. The approach adopted is an exact full-wave method in which all the physical phenomena are taken into account. For simplicity and without the loss the generality, the current source is assumed to be an infinitesimal dipole (δ function). It is of interest to know the phase front and energy distribution at any observation angle, and the different properties of each distinct surface wave modes.

Since surface waves always exist in integrated circuit structures, from both theoretical and practical points of view, it is of interest to study the surface wave properties due to the anisotropy of the ferrite substrate. In Section II, the plane wave representation of electromagnetic fields due to an arbitrarily oriented current source on ferrite substrate are described by using an exponential-matrix method [12]. In Section III, the analysis for extracting surface waves from a continuous plane wave spectrum is discussed. The numerical results for the characteristics of different surface wave modes, including surface wave pole diagrams, equi-phase contours, and power distribution, are shown in Section IV.

II. Fields Due to a δ Source on a Ferrite Substrate—Green's Function

The permeability tensor of biased ferrites is in the form of

$$\bar{\bar{\mu}} = \mu_0[\mathcal{L}]\begin{bmatrix} \mu & j\kappa & 0 \\ -j\kappa & \mu & 0 \\ 0 & 0 & 1 \end{bmatrix}[\mathcal{L}]^T, \tag{1}$$

Manuscript received July 17, 1991; revised December 10, 1991. This work was supported by the U.S. Air Force under contract F19628-91-C-0089.

H.-Y. Yang and J. A. Castaneda are with Phraxos Research & Development Inc., Ocean Park, Blvd., Suite 1020, Santa Monica, CA 90405.

N. G. Alexopoulos is with the Electrical Engineering Department, University of California, Los Angeles, Los Angeles, CA 90066.

IEEE Log Number 9106332.

0018-9480/92$03.00 © 1992 IEEE

where

$$\mu = 1 + \frac{\omega_0\omega_M}{\omega_0^2 - \omega^2}, \quad \kappa = \frac{\omega\omega_M}{\omega_0^2 - \omega^2}, \tag{2}$$

$$\omega_0 = \gamma\mu_0 H_0, \quad \omega_M = \gamma\mu_0 M_s, \tag{3}$$

M_s is the material saturation magnetization, H_0 is the dc magnetic field, $\gamma = 1.759 \times 10^{11}$ kg/coul. Also

$$[\mathfrak{L}] = \begin{bmatrix} \cos\theta_0\cos\phi_0 & \cos\theta_0\sin\phi_0 & -\sin\theta_0 \\ -\sin\phi_0 & \cos\phi_0 & 0 \\ \sin\theta_0\cos\phi_0 & \sin\theta_0\sin\phi_0 & \cos\theta_0 \end{bmatrix}, \tag{4}$$

with the dc magnetic field in the direction of $\hat{N}$, where

$$\hat{N} = \sin\theta_0\cos\phi_0\hat{x} + \sin\theta_0\sin\phi_0\hat{y} + \cos\theta_0\hat{z}. \tag{5}$$

The Green's function for a ferrite substrate does not have a simple analytic form. For the problem of interest, sources are either tangential to the surface of the substrate (microstrip) or perpendicular to the ground plane (probe). This geometry is shown in Fig. 1. Then Maxwell's equations for the fields inside the ferrite slab ($0 < z < d$) are

$$\nabla \times \vec{E} = -j\omega\bar{\mu} \cdot \vec{H}$$

and

$$\nabla \times \vec{H} = j\omega\epsilon_r\vec{E} + \hat{u}\,\delta(x - x')\,\delta(y - y')\,\delta(z - z'), \tag{6}$$

where $\hat{u}$ is a unit vector and x', y' and z' are the source coordinates. If it is assumed that the structure is homogeneous in the planar direction (x-y plane), one may introduce the following Fourier transformation

$$\begin{matrix}\vec{E} \\ \vec{H}\end{matrix} = \frac{1}{4\pi^2}\int_{-\infty}^{\infty} \begin{matrix}\tilde{E} \\ \tilde{H}\end{matrix}(k_x, k_y)\, e^{-jk_x(x - x')} e^{-jk_y(y - y')}\, dk_x\, dk_y. \tag{7}$$

By using (6), one obtains

$$-j\boldsymbol{k} \times \tilde{H} + \frac{\partial}{\partial z}(\hat{z} \times \tilde{H}) = j\omega\epsilon_r \cdot \tilde{E} + \hat{u}\,\delta(z - z') \tag{8}$$

and

$$-j\boldsymbol{k} \times \tilde{E} + \frac{\partial}{\partial z}(\hat{z} \times \tilde{E}) = -j\omega\bar{\mu} \cdot \tilde{H}. \tag{9}$$

With (8) and (9) and after some algebraic manipulations, one may obtain coupled first-order differential equations which in a matrix form are

$$\frac{\partial}{\partial z}[\tilde{\psi}(z)] = [A][\tilde{\psi}(z)] + [U_I]\,\delta(z - z') \tag{10}$$

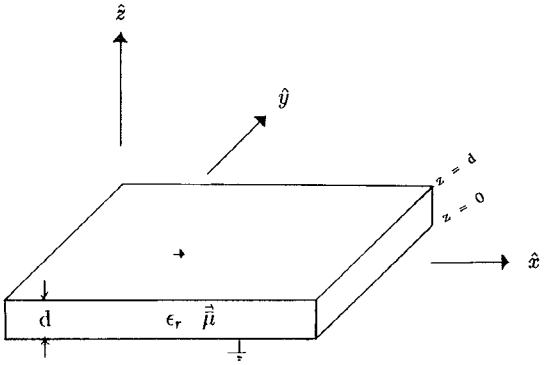

Fig. 1. An elementary source on a ferrite substrate.

where

$$[\tilde{\psi}(z)] = \begin{bmatrix} k_x\tilde{H}_x(z) + k_y\tilde{H}_y(z) \\ k_y\tilde{H}_x(z) - k_x\tilde{H}_y(z) \\ k_x\tilde{E}_x(z) + k_y\tilde{E}_y(z) \\ k_y\tilde{E}_x(z) - k_x\tilde{E}_y(z) \end{bmatrix},$$

$$[A] = \begin{bmatrix} a_{11} & a_{12} & a_{13} & a_{14} \\ a_{21} & a_{22} & a_{23} & a_{24} \\ a_{31} & a_{32} & a_{33} & a_{34} \\ a_{41} & a_{42} & a_{43} & a_{44} \end{bmatrix} \tag{11}$$

and $[U_I]$ is either $[U_x]$, $[U_y]$ or $[U_z]$ and

$$[U_x] = \begin{bmatrix} -k_y \\ k_x \\ 0 \\ 0 \end{bmatrix}, \quad [U_y] = \begin{bmatrix} k_x \\ k_y \\ 0 \\ 0 \end{bmatrix}$$

and

$$[U_z] = \begin{bmatrix} 0 \\ 0 \\ (k_x^2 + k_y^2)/(\omega\epsilon_0\epsilon_r) \\ 0 \end{bmatrix}. \tag{12}$$

$[U_x]$, $[U_y]$ and $[U_z]$ are for the current source in the x, y and z directions respectively. The matrix elements of $[A]$ which is a function of the spectral variables k_x, k_y and material parameters, are shown explicitly in the Appendix. If one defines the 4×4 matrices $[\lambda]$ and $[\tilde{\phi}]$ as

$$[\lambda] = \begin{bmatrix} \lambda_1 & 0 & 0 & 0 \\ 0 & \lambda_2 & 0 & 0 \\ 0 & 0 & \lambda_3 & 0 \\ 0 & 0 & 0 & \lambda_4 \end{bmatrix} \tag{13}$$

and

$$[\tilde{\phi}] = [\vec{\phi}_1, \vec{\phi}_2, \vec{\phi}_3, \vec{\phi}_4], \tag{14}$$

where λ_i and $\vec{\phi}_i$ with $i = 1, 2, 3, 4$ are the eigenvalues and eigenvectors of the matrix $[A]$, the following identities hold.

$$[A][\tilde{\phi}] = [\tilde{\phi}][\lambda] \quad \text{and} \quad [A] = [\tilde{\phi}][\lambda][\tilde{\phi}]^{-1}. \tag{15}$$

Equation (10) can therefore be written as

$$\frac{\partial}{\partial z}([\tilde{\phi}]^{-1}[\tilde{\psi}(z)]) = [\lambda]([\tilde{\phi}]^{-1}[\tilde{\psi}(z)]) + [\tilde{\phi}]^{-1}[U_I]\,\delta(z - z'). \tag{16}$$

As a result, the solution of (10) for $z \neq z'$ is

$$[\tilde{\psi}(z)] = [T(z - z_1)][\tilde{\psi}(z_1)], \tag{17}$$

where

$$[T(z)] = [\tilde{\phi}]\begin{bmatrix} e^{\lambda_1 z} & 0 & 0 & 0 \\ 0 & e^{\lambda_2 z} & 0 & 0 \\ 0 & 0 & e^{\lambda_3 z} & 0 \\ 0 & 0 & 0 & e^{\lambda_4 z} \end{bmatrix}[\tilde{\phi}]^{-1}. \tag{18}$$

It is quite clear that the physical meaning of the matrix $[T]$ is to relate the tangential electromagnetic fields at one surface ($z = z_1$) to another ($z = z_2$). For the geometry shown in Fig. 1, the tangential electromagnetic fields at the air-material interface can now be related to those at the ground plane as

$$[T(z' - d)][\tilde{\psi}(d)] - [T(z')][\tilde{\psi}(0)] = [U_I] \tag{19}$$

or

$$[\tilde{\psi}(d)] - [T(d)][\tilde{\psi}(0)] = [T(d - z')][U_I]. \tag{20}$$

The electromagnetic fields in the air ($z \geq d$) can be derived in a straightforward manner. With this result together with the boundary conditions that the tangential electric fields are zero at the ground plane, one obtains

$$[\tilde{\psi}(d^+)] = \begin{bmatrix} j\sqrt{k^2 - k_0^2}\,\tilde{a} \\ \omega\epsilon_0\tilde{b} \\ j\sqrt{k^2 - k_0^2}\,\tilde{b} \\ -\omega\mu_0\tilde{a} \end{bmatrix}$$

and

$$[\tilde{\psi}(0)] = \begin{bmatrix} \tilde{c} \\ \tilde{d} \\ 0 \\ 0 \end{bmatrix}, \tag{21}$$

where $\tilde{a}$, $\tilde{b}$, $\tilde{c}$ and $\tilde{d}$ are unknown spectral quantities to be determined.

Equation (20) is a matrix equation with four equations and four unknowns, where the solution determines the quantities $\tilde{a}$, $\tilde{b}$, $\tilde{c}$ and $\tilde{d}$. As a result, $[\tilde{\psi}(d^+)]$ and $[\tilde{\psi}(0)]$ are determined. The spectral field components at any z can be found from (21) and the translation matrix $[T(z - z')]$.

III. Surface Waves on Ferrite Substrates

The complete electromagnetic wave spectrum has been derived in Section II. The electromagnetic fields may be written in the following form:

$$\vec{E}(x, y, z) = \int_{-\infty}^{\infty}\int_{-\infty}^{\infty} \frac{\vec{A}(k_x, k_y, z)}{D(k_x, k_y)} \cdot e^{-jk_x x}e^{-jk_y y}\,dk_x\,dk_y \tag{22}$$

and

$$\vec{H}(x, y, z) = \int_{-\infty}^{\infty}\int_{-\infty}^{\infty} \frac{\vec{C}(k_x, k_y, z)}{D(k_x, k_y)} \cdot e^{-jk_x x}e^{-jk_y y}\,dk_x\,dk_y. \tag{23}$$

The surface wave contribution comes from the singularities of the integrand, which are defined by the solutions of $D(k_x, k_y) = 0$. The plots of surface wave pole contours in the spectral (k_x, k_y) plane constitute multiple continuous curves. Each contour corresponds to a surface wave mode. Each surface wave pole contour is found numerically. Using the residue theorem, the surface wave fields can be written as

$$\vec{E}_s(x, y, z) = -\pi j \sum_i \int \frac{\vec{A}_p^i(k_x, z)}{D_p^i(k_x)} \cdot e^{-jk_x x}e^{-jf_i(k_x)y}\,dk_x \tag{24}$$

and

$$\vec{H}_s(x, y, z) = -\pi j \sum_i \int \frac{\vec{C}_p^i(k_x, z)}{D_p^i(k_x)} \cdot e^{-jk_x x}e^{-jf_i(k_x)y}\,dk_x, \tag{25}$$

where

$$\vec{A}_p^i(k_x, z) = \vec{A}(k_x, k_y, z)|_{k_y = f_i(k_x)}, \tag{26}$$

$$\vec{C}_p^i(k_x, z) = \vec{C}(k_x, k_y, z)|_{k_y = f_i(k_x)}, \tag{27}$$

$$D_p^i(k_x) = \frac{\partial}{\partial k_y} D(k_x, k_y)|_{k_y = f_i(k_x)}, \tag{28}$$

and $k_y = f_i(k_x)$ is the functional form of the roots of $D(k_x, k_y) = 0$ with $i = 1, 2, \cdots$. With the coordinate transformation

$$x = \rho\cos\phi \quad \text{and} \quad y = \rho\sin\phi, \tag{29}$$

and with the saddle point method [13], the surface wave far fields ($\rho >> 1$) are

$$\vec{E}_s(\rho, \phi, z) = \frac{(\pm 1 - j)\pi\sqrt{\pi}}{2\sqrt{\rho}} \sum_i \frac{\vec{A}_p^i(k_p^i, z)}{D_p^i(k_p^i)} \cdot \frac{e^{[-j\rho(k_p^i\cos\phi + f_i(k_p^i)\sin\phi)]}}{\sqrt{|f_i''(k_p^i)\sin\phi|}} \tag{30}$$

and

$$\vec{H}_s(\rho, \phi, z) = \frac{(\pm 1 - j)\pi\sqrt{\pi}}{2\sqrt{\rho}} \sum_i \frac{\vec{C}_p^i(k_p^i, z)}{D_p^i(k_p^i)} \cdot \frac{e^{[-j\rho(k_p^i\cos\phi + f_i(k_p^i)\sin\phi)]}}{\sqrt{|f_i''(k_p^i)\sin\phi|}}, \tag{31}$$

where the saddle points k_p^i with $i = 1, 2, \cdots$ are the solutions of

$$\frac{df_i(k_x)}{dk_x} = -\cot\phi. \tag{32}$$

The equiphase plane is

$$\rho(k_p^i\cos\phi + f_i(k_p^i)\sin\phi) = \text{constant}. \tag{33}$$

The power density in a particular direction ϕ is

$$P(\phi) = \frac{\text{Re}}{2}\int_0^\infty (\vec{E}_s \times \vec{H}_s^* \cdot \hat{\rho})\rho\, dz. \tag{34}$$

IV. Result Discussions

Surface waves in a grounded substrate propagate along the material-air interface and decay exponentially toward free space. For isotropic substrates, surface waves are cylindrical plane waves and are either TM or TE modes. For anisotropic substrates, surface waves are no longer in a TE or TM form. Moveover, due to the asymmetry of the material anisotropy, the wave front is not of a cylindrical shape.

For two-dimensional surface waves with no variation in y and biased field in the y direction, the fields are in the following forms [5]:

$$\vec{E} \sim \vec{f}(z)e^{-j\beta x} \tag{35}$$

and

$$\vec{H} \sim \vec{g}(z)e^{-j\beta x} \tag{36}$$

with the characteristic equation for TM modes

$$\mu q \coth(q\,d) = \beta\kappa - (\mu^2 - \kappa^2)\sqrt{\beta^2 - k_0^2}, \tag{37}$$

and the characteristic equation for TE modes

$$\epsilon_r\sqrt{\beta^2 - k_0^2}\coth(q_1\,d) = -q_1, \tag{38}$$

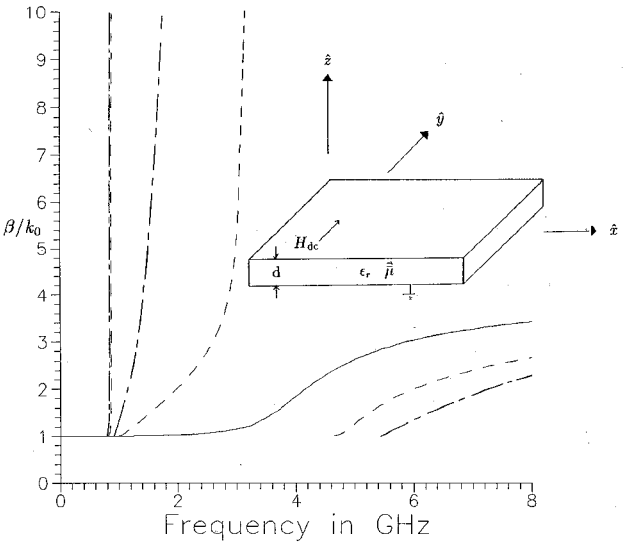

Fig. 2. Surface wave modes of a grounded ferrite slab. $d = 0.5$ cm, $\epsilon_r = 15$, $H_{dc} = 100$ G, $M_s = 10H_{dc}$. ———TM mode;—— TE modes waves propagate along $+\hat{x}$; ---- TE modes waves propagate along $-\hat{x}$.

where

$$q = \sqrt{\beta^2 + k_0^2\epsilon_r(\kappa^2/\mu - \mu)} \tag{39}$$

and

$$q_1 = \sqrt{\beta^2 - k_0^2\epsilon_r}. \tag{40}$$

An example of the dispersion curve is shown in Fig. 2. It is seen that there exist four modes with a resonance where the propagation constants are infinitely large. These modes are similar to the solutions of the Laplace equation for the magnetic potential and are often called magnetostatic wave modes. The TM mode with no cut-off frequency is identical to that of a dielectric slab, while the TE modes that turn on at higher frequencies have characteristics similar to those of the TE modes of a dielectric slab. These modes are called dynamic surface wave modes. The magneto-static wave modes exist in the frequency range of $\sqrt{\omega_0(\omega_0 + \omega_m)} \le \omega \le \omega_0 + \omega_m$.

Surface waves due to a dipole current on a ferrite substrate can be described in terms of a continuous plane wave spectrum. The plane-wave ferrite modes described above are a spectral component of the continuous spectrum ($k_y = 0$, $k_x = \beta$). From the derivation of the surface waves in Section III, it is seen that the surface wave pole contour plays an important role in determining the properties of the surface waves in the far zone. The slope at any position of the contour corresponds to an observation angle ϕ. At this position, the spectral variables k_x and k_y determine the plase constant of the waves, and the second derivative is related to the strength of the fields at that particular angle ϕ.

The numerical results are for the case of a ferrite substrate with thickness of 5 mm, dielectric constant 15, saturation magnetization of 1000 G, bias H field of 100 G. The direction of the bias field is assumed in the $\hat{y}$ direction. The dominant surface wave mode for an isotropic

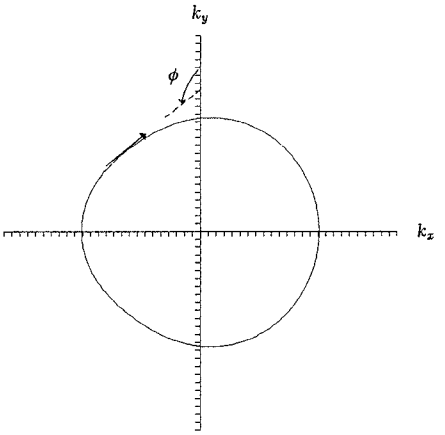

Fig. 3. Surface-wave pole contour of the fundamental mode.

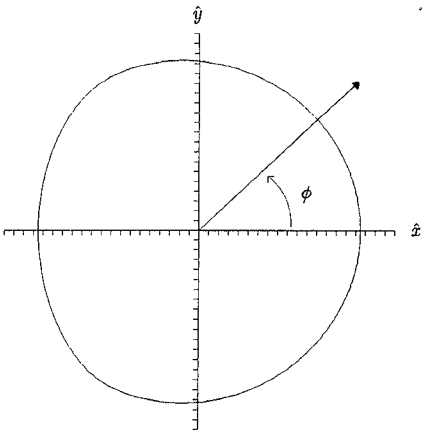

Fig. 4. Equi-phase plane of the fundamental mode at $\mathbf{Z}$ = constant.

substrate is a TM mode, whose equiphase plane is a circular cylinder. For a ferrite substrate, the surface wave pole contour and the equi-phase plane of the fundamental mode are shown in Figs. 3 and 4, respectively. The fundamental mode is a dynamic mode which is similar to the TM mode for an isotropic substrate. It is seen that the dynamic surface wave pole contour is a closed contour and that the slope at each point of the contour corresponds to an observation angle. Since the slope varies from $-\infty$ to ∞, according to (32), the equi-phase plane at any z covers the entire region (ϕ varies from 0 to 2π). The procedure for finding the phase front from the surface wave pole contour can be described as follows: First, one starts at any point on the contour (k_x, k_y) and finds the slope at that point. Then from the slope, one finds the observation angle ϕ. The phase constant at that observation angle is $k_x \cos \phi + k_y \sin \phi$. It is seen from Fig. 4 that for a $\hat{y}$ directed bias field, the fundamental mode has a smaller propagation constant in the positive x direction than in the negative x direction. Also, for the bias field in the $\hat{y}$ direction, the surface wave is symmetric with respect to the $\hat{x}$ axis. This phenomenon exists due to the symmetry of the permeability tensor and is true for all waves including radiated waves as well as the dominant and higher order surface waves. The equiphase plane is otherwise quite irregular. The power density is defined as the total power in any ϕ direction per radian. The surface wave power pattern for an isotropic substrate is a figure eight. The power density patterns for the fundamental mode of a ferrite substrate are shown in Figs. 5 and 6 for the current in the $\hat{x}$ and $\hat{y}$ directions, respectively. It is seen from Figs. 5 and 6 that due to the bias field, the power pattern of the first surface wave mode of a ferrite substrate may be highly directive, especially when the bias field is in the same direction as the current source. The direction of the main beam may be controlled by the strength of the bias field. This phenomenon may find applications for surface wave antennas. It is also seen that the angle where the power pattern has a null moves with the change of the direction of the bias field. For the source in the $\hat{x}$ direction

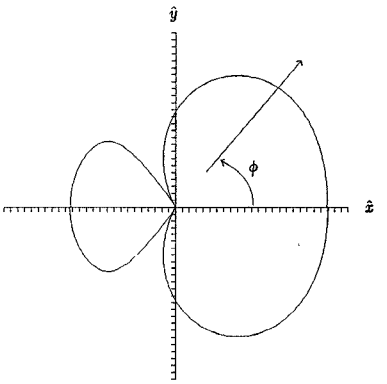

Fig. 5. Power pattern of the fundamental mode. d = 0.5 cm, ϵ_r = 15, H_{dc} = 100 G, $M_s = 10H_{dc}$, F = 6 GHz. Biased H field in the y direction, current in the x direction.

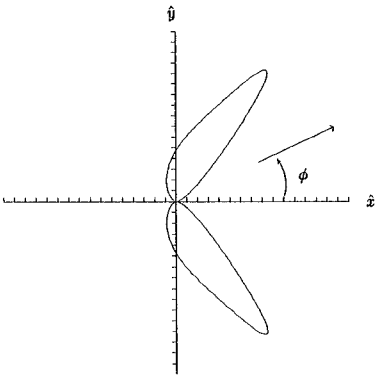

Fig. 6. Power pattern of the fundamental mode. d = 0.5 cm, ϵ_r = 15, H_{dc} = 100 G, $M_s = 10H_{dc}$, F = 6 GHz. Biased H field in the y direction, current in the y direction.

and the bias field in the $\hat{y}$ direction, there is more surface wave power in the $\hat{x}$ than in the $-\hat{x}$ direction.

The surface wave mode with a closed pole contour described above is similar to the surface wave modes of an isotropic substrate. However, for a current source on ferrite substrate, it is found that there may exist additional surface wave modes. These three-dimensional surface

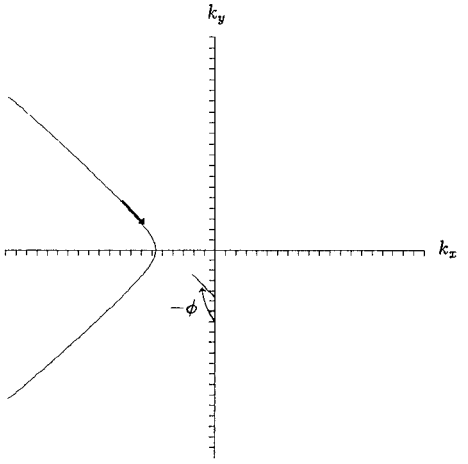

Fig. 7. Pole contour of a magneto-static wave mode.

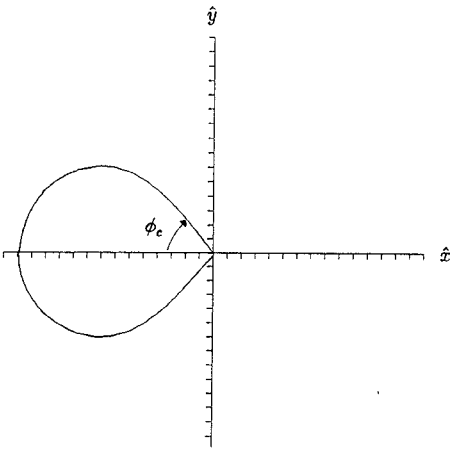

Fig. 8. Equi-phase contour of a magneto-static wave mode.

wave modes corresponds to the magneto-static wave modes found in two dimensional plane wave structures and here are called magneto-static waves. An example of the pole contour of a magneto-static wave mode is shown in Fig. 7. It is seen that the pole contour is not closed and is shaped like a parabola. This is true for all the magneto-static waves. The pole contour shown in Fig. 7 is for the magneto-static wave which propagates toward the left-hand side of the bias field. It is also seen that the pole contour is asymptotically a straight line. Since the slope at each point in the contour corresponds to an observation angle, the slope of the straight line gives the upper or lower bounds of the observation angle. This implies that there is only a certain range of angles ϕ where this magneto-static wave may propagate. There exists a critical angle ϕ_c which distinguishes the shadow region and the illuminated region. The corresponding equi-phase contour of this magneto-static wave mode is shown in Fig. 8. It is seen from Fig. 8 that outside the region of $\pi - \phi_c \leq \phi \leq \pi + \phi_c$, the phase of the waves is always zero, which means that the wave propagates infinitely slowly or simply does not propagate. The critical angle ϕ_c is a function of ferrite material parameters and the strength of the bias field, and is not a function of the thickness of the substrate. The power density of the magneto-static wave mode as a function of the observation angle ϕ is shown in Fig. 9. It is interesting to see that the power is mostly confined near the shadow region boundaries.

The pole contour of a magneto-static wave mode propagating toward the right-hand side of the bias field is shown in Fig. 10. The equi-phase contour and the power pattern are shown in Fig. 11 and Fig. 12, respectively. Since the bias field is assumed in the $\hat{y}$ direction, the waves are symmetric to the x axis and asymmetric to the y axis. Therefore, the magneto-static wave propagating toward the left-hand side is very much different from the wave propagating toward the right-hand side. It is seen from Fig. 10, that the pole contour is asymptotically a straight line but with a different slope from that of Fig. 7. Also, the critical angle beyond which the waves can not propagate is different. It is seen from Fig. 11 that the power pattern has very high directivity close to the critical angle. Mathematically, it is found that the observation angle which exhibits such high directivity corresponds to a point in the pole contour which is almost an inflection point (the second derivative is zero).

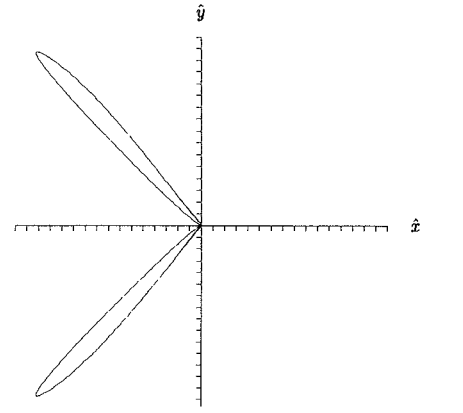

Fig. 9. Power pattern of a magneto-static wave mode. $d = 0.5$ cm, $\epsilon_r = 15$, $H_{dc} = 100$ G, $M_s = 10H_{dc}$, $F = 2.5$ GHz. Biased field in the y direction, current in the x direction.

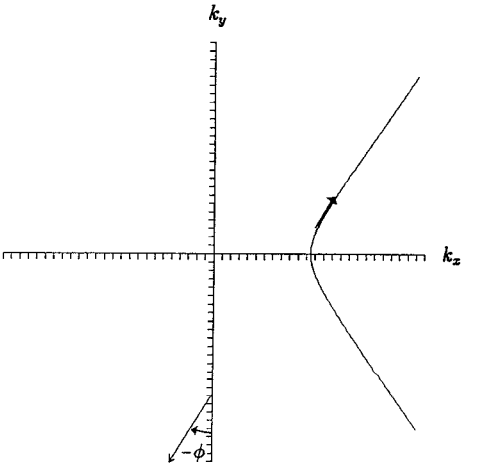

Fig. 10. Pole contour of a magneto-static wave mode.

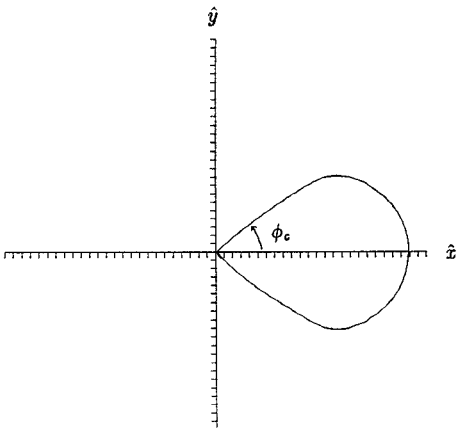

Fig. 11. Equi-phase contour of a magneto-static wave mode.

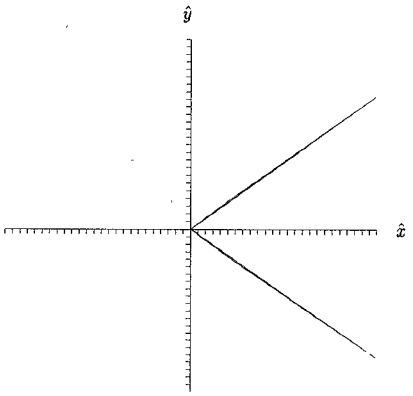

Fig. 12. Power pattern of a magneto-static wave mode. $d = 0.5$ cm, $\epsilon_r = 15$, $H_{dc} = 100$ G, $M_s = 10H_{dc}$, $F = 1.2$ GHz. Biased H field in the y direction, current in the x direction.

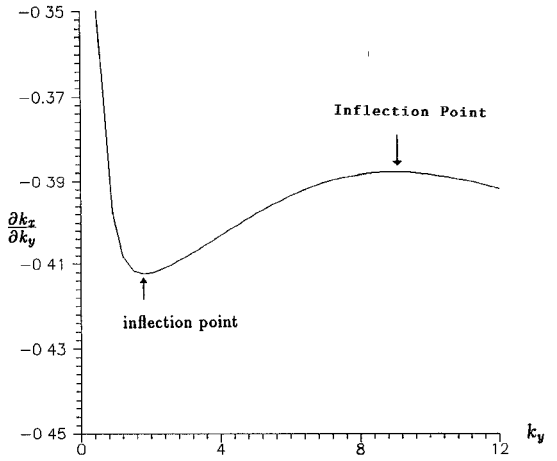

Fig. 13. The slope of the pole contour of a magneto-static wave mode. $d = 0.5$ cm, $\epsilon_r = 15$, $H_{dc} = 100$ G, $M_s = 10H_{dc}$, $F = 1.5$ GHz. Biased H field in the y direction, current in the x direction.

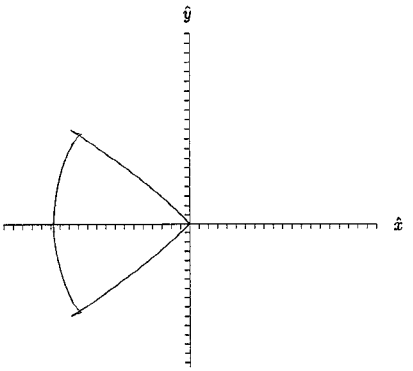

Fig. 14. Equi-phase contour of a magneto-static wave mode with inflection points.

In fact, the inflection points on the pole contour may exist. An example is shown in Fig. 13. It is seen that the slope of the pole contour may not always increase or decrease monotonically. When an inflection point occurs, the asymtotic forms of the surface wave fields in (30) and (31) are no longer valid. The inflection point is a second-order saddle point where the corresponding observation angle is still determined by (32); however the surface wave fields are in the following forms:

$$\vec{E}_s(\rho, \phi, z) = \sqrt[3]{6}\Gamma\left(\frac{1}{3}\right)\frac{(\pm 1 + j\sqrt{3})\pi}{6\sqrt[3]{\rho}}\sum_i \frac{\vec{A}_p^i(k_p^i, z)}{D_p^i(k_p^i)} \cdot \frac{\exp\left[-j\rho\left(k_p^i \cos\phi + f_i(k_p^i)\sin\phi\right)\right]}{\sqrt[3]{\left|f_i^{(3)}(k_p^i)\sin\phi\right|}} \tag{41}$$

and

$$\vec{H}_s(\rho, \phi, z) = \sqrt[3]{6}\Gamma\left(\frac{1}{3}\right)\frac{(\pm 1 + j\sqrt{3})\pi}{6\sqrt[3]{\rho}}\sum_i \frac{\vec{C}_p^i(k_p^i, z)}{D_p^i(k_p^i)} \cdot \frac{\exp\left[-j\rho\left(k_p^i \cos\phi + f_i(k_p^i)\sin\phi\right)\right]}{\sqrt[3]{\left|f_i^{(3)}(k_p^i)\sin\phi\right|}}. \tag{42}$$

It is seen that at the observation angle where the inflection point occurs, the surface waves decay as $1/\sqrt[3]{\rho}$ instead of $1/\sqrt{\rho}$. Therefore the surface waves at these particular angles do not satisfy the radiation condition. However, the total energy passing through any cylinder with radius ρ is still finite, even though the power density at these particular angles is very high. Another interesting phenomenon associated with the inflection point is that the waves may propagate with several phase constants. From the results shown in Figs. 13 and 14, it is possible to have three different propagation constants at one observation angle.

V. Conclusion

In this work, we study the surface waves modes of a gyrotropic substrate due to a small electric dipole. The surface wave modes propagating laterally are extracted from the continuous plane wave spectrum by using the residue theorem and the method of steepest descent. It was found that there exist two distinct types of surface wave modes. The dynamic surface wave modes which are similar to the modes found for a dielectric substrate exist for any direction of biasing and current orientation, and the pole contours in the spectral plane are always closed. The wave number at any observation angle ϕ is always

finite, bounded, and nonzero. The magneto-static modes which arise due to the material properties of ferrite, exist only for transverse biasing and horizontal current sources, and the pole contours in the spectral plane are always open and unbounded. There exist an angular region where waves may propagate. Outside this region, the magnetostatic waves do not exist. For ferrite substrates, the surface wave pole contour may have inflection points and at the corresponding observation angles ϕ, the waves decay as $1/\sqrt[3]{\rho}$ instead of $1/\sqrt{\rho}$. In this case, the energy is highly concentrated near the inflection angle. Also it was found that if the pole contour has inflection points, the waves propagating at an angle ϕ may have multiple phase constants.

Appendix

The matrix elements of $[A]$ defined in (11) are

$$a_{11} = \frac{j}{\mu_{zz}}(k_x\mu_{zx} + k_y\mu_{zy}), \quad a_{12} = \frac{j}{\mu_{zz}}(k_y\mu_{zx} - k_x\mu_{zy}),$$

$$a_{13} = 0, \quad a_{14} = \frac{j\omega\epsilon_0 k^2}{k_0^2\mu_{zz}} + \frac{j\omega\epsilon_0}{k^2} - \epsilon_r(k_x^2 + k_y^2)$$

$$a_{21} = 0, \quad a_{22} = 0,$$

$$a_{23} = \frac{j\omega\epsilon_0}{k^2}\epsilon_r(k_x^2 + k_y^2), \quad a_{24} = 0,$$

$$a_{31} = \frac{j\omega\mu_0}{k^2}\left[\mu_{xy}k_y^2 - \mu_{yx}k_x^2 + (\mu_{xx} - \mu_{yy})k_xk_y - \frac{k_y\mu_{xz} - k_x\mu_{yz}}{\mu_{zz}}(k_y\mu_{zx} + k_x\mu_{zy})\right],$$

$$a_{32} = \frac{-j\omega\mu_0 k^2}{k_0^2\epsilon_{zz}} + \frac{j\omega\mu_0}{k^2}\left[\mu_{yy}k_x^2 + \mu_{xx}k_y^2 - (\mu_{xy} + \mu_{yx})k_xk_y - \frac{k_y\mu_{xz} - k_x\mu_{yz}}{\mu_{zz}} \cdot (k_y\mu_{zx} - k_x\mu_{zy})\right],$$

$$a_{33} = 0, \quad a_{34} = -\frac{j}{\mu_{zz}}(k_y\mu_{xz} - k_x\mu_{yz}),$$

$$a_{41} = \frac{-j\omega\mu_0}{k^2}\left[\mu_{xx}k_x^2 + \mu_{yy}k_y^2 + (\mu_{xy} + \mu_{yx})k_xk_y - \frac{k_y\mu_{yz} + k_x\mu_{xz}}{\mu_{zz}}(k_y\mu_{zy} + k_x\mu_{zx})\right],$$

$$a_{42} = \frac{-j\omega\mu_0}{k^2}\left[-\mu_{xy}k_x^2 + \mu_{yx}k_y^2 + (\mu_{xx} - \mu_{yy})k_xk_y - \frac{k_y\mu_{yz} + k_x\mu_{xz}}{\mu_{zz}}(k_y\mu_{zx} - k_x\mu_{zy})\right],$$

$$a_{43} = 0, \quad a_{44} = \frac{j}{\mu_{zz}}(k_x\mu_{xz} + k_y\mu_{yz}).$$

References

[1] D. Polder, "On the theory of ferromagnetic resonance," *Phil. Mag.*, vol. 40, pp. 99–115, 1949.

[2] R. E. Collin, *Foundations for Microwave Engineering*. New York: McGraw-Hill, 1966, pp. 286–294.

[3] P. B. Katehi and N. G. Alexopoulos, "On the effect of substrate thickness and permittivity on printed circuit dipole properties," *IEEE Trans. Antennas Propagat.*, vol. AP-31, no. 1, pp. 34–39, Jan. 1983.

[4] R. W. Damon and J. R. Eshbach, "Magnetostatic modes of a ferromagnetic slab," *J. Phys. Chem. Solids*, vol. 19, pp. 308–320, 1961.

[5] S. R. Seshadri, "Surface magnetostatic modes of a ferrite slab," *Proc. IEEE* (Lett.), vol. 58, pp. 506–507, Mar. 1970.

[6] R. E. De Wames and T. Wolfram, "Characteristics of magnetostatic surface waves for a metalized ferrite slab," *J. Appl. Phys.*, vol. 41, pp. 5243–5246, 1970.

[7] T. J. Gerson and J. S. Nadan, "Surface electromagnetic modes of a ferrite slab," *IEEE Trans. Microwave Theory Tech.*, vol. MTT-22, pp. 757–762, Aug. 1974.

[8] A. K. Ganguly and D. C. Webb, "Microstrip excitation of magnetostatic surface waves: theory and experiment," *IEEE Trans. Microwave Theory Tech.*, vol. MTT-22, pp. 998–1006, Dec. 1975.

[9] A. Karsono and D. Tilley, "Retarded electromagnetic modes in a ferromagnetic slab," *J. Phys. C. Solid State Physics*, vol. 11, pp. 3487–3492, 1978.

[10] R. Ruppin, "Electromagnetic modes of a ferromagnetic slab," *J. Appl. Phys.*, vol. 62(1), pp. 11–15, July, 1987.

[11] L. B. Goldberg, "Excitation of surface magnetostatic waves by a point current element," *Sov. Phys. Tech. Phys* , vol. 31, pp. 1132–1137, Oct. 1986.

[12] M. A. Morgan, D. L. Fisher, and E. A. Miline, "Electromagnetic scattering by stratified inhomogeneous anisotropic media," *IEEE Trans. Antennas Propagat.*, vol. AP-35, no. 2, pp. 191–197, Feb. 1987.

[13] R. E. Collin, *Field Theory of Guided Waves*. New York: McGraw-Hill, 1960, pp. 495–506.

Hung-Yu Yang, (S'87–M'88) was born in Taipei, Taiwan, on October 25, 1960. He received the B.S. degree in electrical engineering from the National Taiwan University in 1982 and the M.S. and Ph.D. degrees in electrical engineering from the University of California, Los Angeles, in 1985 and 1988, respectively.

His research has focused on millimeter-wave printed circuit antennas, printed antenna design, and the modeling of millimeter-wave integrated circuit discontinuities. Currently he is a Research Engineer with Phraxos Research and Development, Inc., Santa Monica, CA. There he is involved in the development of computer codes for frequency selective surfaces, computer-aided design of high-frequency integrated circuit discontinuities, the synthesis of microstrip arrays, and scattering from antennas.

Jesse A. Castaneda, (S'83–M'86) received the B.S. degree in physics in 1970 from Saint Mary's College of California. He then received the M.S.E.E. degree in 1978, the engineer degree in 1980, and the Ph.D. degree in electrical engineering in 1988, all from the University of California at Los Angeles.

From 1978 through 1983 he was with the Radar Systems Group of the Hughes Aircraft Company. Since 1986 he has been with Phraxos Research and Development, Inc., of Santa Monica, CA, where he is Vice President. Dr. Castaneda has worked in the field of microwave antennas with experience in the areas of phased arrays, planar arrays, frequency selective surfaces and radomes, and adaptive arrays. His current interests are in the area of microstrip circuit and microstrip antenna CAD.

Nicolaos G. Alexopoulos, (S'68–M'69–SM'82–F'87) graduated from the 8th Gymnasium of Athens, Greece, and received the B.S.E.E., M.S.E.E., and Ph.D. degrees from the University of Michigan, Ann Arbor, in 1964, 1967, and 1968, respectively.

Currently he is Professor and Chairman of the Electrical Engineering Department at the University of California, Los Angeles. He is also a Consultant with Northrop Corporation's Advanced Systems Division. His current research interests are in electromagnetic theory as it applies to the modeling of integrated-circuit components and printed circuit antennas for microwave and millimeter-wave applications, substrate materials and their effect on integrated-circuit structures and printed antennas, integrated-circuit antenna arrays, and antenna scattering studies. He is also interested in the interaction of electromagnetic waves with materials, in particular, active media.

Dr. Alexopoulos is an Associate Editor of the journals *Electromagnetics* and *Alta Frequenza* and is on the Editorial Boards of the IEEE TRANSACTIONS ON MICROWAVE THEORY AND TECHNIQUES and the *International Journal on Electromagnetic Theory*. He served as the 1974 Chairman of the IEEE AP-S Chapter. He was a corecipient (Honorable Mention) of the 1983 AP-S R.W.P. King Best Paper Award.